Romanian Reports in Physics **70**, 404 (2018)

APPLICATION OF A TRANSFER MATRIX METHOD TO HOLLOW-CORE BRAGG FIBER WITH A GOLD LAYER

V.A. POPESCU

Politehnica University of Bucharest, Department of Physics 1, 313 Splaiul Independentei, 060042 Bucharest, Romania
E-mail: vapopescu@yahoo.com

Received June 8, 2017

Abstract. For a hollow-core Bragg fiber, the field is represented by a Bessel function of the first kind in the core region, a linear combination of Bessel functions of the first and second kinds in the dielectric interior layers, a linear combination of the Hankel functions in the gold region and a Hankel function of the first kind in the external infinite medium. Our analytical method is applied for different structures made from 19, 11, and 5 layers. When a high index material just before the outermost region of a hollow-core Bragg fiber is replaced by a gold layer, the optical confinement for the TE_{01} mode in the core is increased about ten times. If the gold layer is located between the first and the penultimate layer, the loss for the same mode is increased.

Key words: sensors, hollow-core fibers, surface plasmon resonance, finite element method.

1. INTRODUCTION

The transfer matrix method has been used over the past decades for the analysis of planar waveguides [1], optical fibers [2–5], fiber gratings [6–7], and fiber based plasmonic sensors [8–11].

The solutions of the wave equation with cylindrical symmetry for the electric field $\vec{E}$ and the magnetic field $\vec{H}$ in the fiber yield to a dependency in the form $e^{-i\beta z}$ in the z direction and $e^{i\nu\varphi}$ around the circumference of the fiber, and to the radial solutions Ψ and Φ [3]:

$$\vec{E} = [(\frac{1}{r}\frac{\partial\Psi}{\partial\varphi} - \frac{\beta}{\omega\varepsilon_0 n^2}\frac{\partial\Phi}{\partial r})\vec{1}_r - (\frac{\partial\Psi}{\partial r} + \frac{\beta}{\omega\varepsilon_0 n^2 r}\frac{\partial\Phi}{\partial\varphi})\vec{1}_\varphi - (\frac{k^2n^2-\beta^2}{i\omega\varepsilon_0 n^2})\Phi\vec{1}_z]e^{-i\beta z}, \tag{1}$$

and

$$\vec{H} = [(\frac{1}{r}\frac{\partial\Phi}{\partial\varphi} + \frac{\beta}{\omega\mu_0}\frac{\partial\Psi}{\partial r})\vec{1}_r + (-\frac{\partial\Phi}{\partial r} + \frac{\beta}{\omega\mu_0 r}\frac{\partial\Psi}{\partial\varphi})\vec{1}_\varphi + (\frac{k^2n^2-\beta^2}{i\omega\mu_0})\Psi\vec{1}_z]e^{-i\beta z}, \tag{2}$$

where μ_0 is the free space magnetic permeability, ε_0 is the vacuum permittivity, ω is the angular frequency, $\vec{1}_r$, $\vec{1}_\varphi$, and $\vec{1}_z$ are the unit radial, tangential, and axial vectors and the mode index ν must be an integer to ensure periodic solutions with period 2π. For a hollow-core Bragg fiber, the radial solutions Ψ and Φ are represented by a Bessel function of the first kind (J) in the core region, a linear combination of Bessel functions of the first and second kinds (J and Y) in the dielectric interior layers, a linear combination of the Hankel functions (H_1 and H_2) in the gold region, and a Hankel function of the first kind H_1 in the external infinite medium. The continuity conditions require that the tangential components φ and z of the electric field E and the magnetic field H must be matched at the different layer interfaces.

A low loss of the TE_{01} mode in a hollow-core Bragg fiber with large radius was obtained by using a high contrast for the refractive indices (n_1 =1, n_2 = 4.6, n_3 = 1.6, n_{N-1} = 4.6, n_N = 1.6) of the alternating layers [12], where N is the number of the layers.

In the proposed device, the high index material just before the outermost region of a hollow-core Bragg fiber is replaced by a gold layer and the optical confinement in the core is increased about ten times.

2. ANALYTICAL METHOD FOR A HOLLOW-CORE BRAGG FIBER WITH A GOLD LAYER

For a hollow-core Bragg fiber with five layers, we have [5, 8]:

$$M_0\begin{pmatrix}A_1\\B_1\\C_1\\D_1\end{pmatrix} = M_1\begin{pmatrix}A_2\\B_2\\C_2\\D_2\end{pmatrix}; M_2\begin{pmatrix}A_2\\B_2\\C_2\\D_2\end{pmatrix} = M_3\begin{pmatrix}A_3\\B_3\\C_3\\D_3\end{pmatrix}; \tag{3}$$

$$M_4\begin{pmatrix}A_3\\B_3\\C_3\\D_3\end{pmatrix} = M_5\begin{pmatrix}A_4\\B_4\\C_4\\D_4\end{pmatrix}; M_6\begin{pmatrix}A_4\\B_4\\C_4\\D_4\end{pmatrix} = M_f\begin{pmatrix}A_5\\B_5\\C_5\\D_5\end{pmatrix}; \tag{4}$$

$$M_4\begin{pmatrix}A_3\\B_3\\C_3\\D_3\end{pmatrix}=M_{5g}\begin{pmatrix}A_4\\B_4\\C_4\\D_4\end{pmatrix};M_{6g}\begin{pmatrix}A_4\\B_4\\C_4\\D_4\end{pmatrix}=M_f\begin{pmatrix}A_5\\B_5\\C_5\\D_5\end{pmatrix},\tag{5}$$

where the index g refers to a gold layer and the elements of the matrices M_0, M_1, M_2, M_3, M_4, M_5, M_{5g}, M_6, M_{6g} , and M_f are

$$M_0^{11}=-\frac{u_1^2}{n_1^2}J_\nu(u_1r_1),M_0^{12}=0,M_0^{13}=0,M_0^{14}=0,\tag{6}$$

$$M_0^{21}=-J_\nu{}'(u_1r_1),M_0^{22}=0,M_0^{23}=\frac{i\nu\beta}{\omega\mu_0r_1}J_\nu(u_1r_1),M_0^{24}=0,\tag{7}$$

$$M_0^{31}=0,M_0^{32}=0,M_0^{33}=u_1^2J_\nu(u_1r_1),M_0^{34}=0,\tag{8}$$

$$M_0^{41}=-\frac{i\nu\beta}{\omega\varepsilon_0n_1^2r_1}J_\nu(u_1r_1),M_0^{42}=0,M_0^{43}=-J_\nu{}'(u_1r_1),M_0^{44}=0,\tag{9}$$

$$M_1^{11}=-\frac{u_2^2}{n_2^2}J_\nu(u_2r_1),M_1^{12}=-\frac{u_2^2}{n_2^2}Y_\nu(u_2r_1),M_1^{13}=0,M_1^{14}=0,\tag{10}$$

$$M_1^{21}=-J'_\nu(u_2r_1),M_1^{22}=-Y'_\nu(u_2r_1),\tag{11}$$

$$M_1^{23}=\frac{i\nu\beta}{\omega\mu_0r_1}J_\nu(u_2r_1),M_1^{24}=\frac{i\nu\beta}{\omega\mu_0r_1}Y_\nu(u_2r_1),\tag{12}$$

$$M_1^{31}=0,M_1^{32}=0,M_1^{33}=u_2^2J_\nu(u_2r_1),M_1^{34}=u_2^2Y_\nu(u_2r_1),\tag{13}$$

$$M_1^{41} = -\frac{i\nu\beta}{\omega\varepsilon_0 n_2^{\,2} r_1} J_\nu(u_2 r_1)\,, M_1^{42} = -\frac{i\nu\beta}{\omega\varepsilon_0 n_2^{\,2} r_1} Y_\nu(u_2 r_1)\,,$$
$$M_1^{43} = -J'_\nu(u_2 r_1)\,, \tag{14}$$

$$M_1^{44} = -Y'_\nu(u_2 r_1)\,, \tag{15}$$

$$M_2 = M_1(r_1 \to r_2)\,, \tag{16}$$

$$M_3 = M_1(r_1 \to r_2, u_2 \to u_3, n_2 \to n_3)\,, \tag{17}$$

$$M_4 = M_1(r_1 \to r_3, u_2 \to u_3, n_2 \to n_3)\,, \tag{18}$$

$$M_5 = M_1(r_1 \to r_3, u_2 \to u_4, n_2 \to n_4)\,, \tag{19}$$

$$M_{5,g} = M_1(r_1 \to r_3, u_2 \to u_4, n_2 \to n_4, J_\nu \to H_{1\nu}, Y_\nu \to H_{2\nu})\,, \tag{20}$$

$$M_6 = M_1(r_1 \to r_4, u_2 \to u_4, n_2 \to n_4)\,, \tag{21}$$

$$M_{6,g} = M_1(r_1 \to r_4, u_2 \to u_4, n_2 \to n_4, J_\nu \to H_{1\nu}, Y_\nu \to H_{2\nu})\,, \tag{22}$$

$$M_f^{11} = 0\,, M_f^{12} = -\frac{w_5^{\,2}}{n_5^{\,2}} H_{1\nu}(w_5 r_4)\,, M_f^{13} = 0\,, M_f^{14} = 0\,, \tag{23}$$

$$M_f^{21} = 0, M_f^{22} = -H_{1\nu}'(w_5 r_4), M_f^{23} = 0,$$
$$M_f^{24} = \frac{i\nu\beta}{\omega\mu_0 r_4} H_{1\nu}(w_5 r_4), \tag{24}$$

$$M_f^{31} = 0, M_f^{32} = 0, M_3^{33} = 0, M_f^{34} = w_4^2 K_\nu(w_4 r_3), \tag{25}$$

$$M_f^{41} = 0, M_f^{42} = -\frac{i\nu\beta}{\omega\varepsilon_0 n_5^2 r_4} H_{1\nu}(w_5 r_4), M_f^{43} = 0,$$
$$M_f^{44} = -H_{1\nu}'(w_5 r_4), \tag{26}$$

where

$$u_1 = \sqrt{(kn_1)^2 - \beta^2}, \; u_2 = \sqrt{(kn_2)^2 - \beta^2}, \; u_3 = \sqrt{(kn_3)^2 - \beta^2}, \tag{27}$$

$$u_4 = \sqrt{(kn_4)^2 - \beta^2}, \; w_5 = \sqrt{(kn_5)^2 - \beta^2}, \tag{28}$$

and where prime represents the differentiation with respect to the radial variable r:

$$F_\nu'(u_i r_j) = \frac{u_i}{2}\{F_{\nu-1}(u_i r_j) - F_{\nu+1}(u_i r_j)\}, F = J, Y, H_1, H_2. \tag{29}$$

The complex propagation constant $\beta = \beta_r + i\,\beta_i$, at a modal index ν is determined from the dispersion equation – the determinant (Δ) formed by the coefficients A_1, C_1, B_4, and D_4 of the equations

$$-\frac{u_1^2}{n_1^2} J_\nu(u_1 r_1) A_1 - B_{12\nu} B_5 - B_{14\nu} D_5 = 0, \tag{30}$$

$$-J'_\nu(u_1 r_1) A_1 + \frac{i\nu\beta}{\omega\mu_0 r_1} J_\nu(u_1 r_1) C_1 - B_{22\nu} B_5 - B_{24\nu} D_5 = 0, \tag{31}$$

$$u_1^2 J_\nu(u_1 r_1) C_1 - B_{32\nu} B_5 - B_{34\nu} D_5 = 0, \tag{32}$$

$$-\frac{i\nu\beta}{\omega\varepsilon_0 n_1^2 r_1} J_\nu(u_1 r_1) A_1 - J'_\nu(u_1 r_1) C_1 - B_{42\nu} B_5 - B_{44\nu} D_5 = 0, \tag{33}$$

must vanish:

$$\Delta = 0, \tag{34}$$

where

$$\Delta = \begin{vmatrix} -\frac{u_1^2}{n_1^2} J_\nu(u_1 r_1) & 0 & -B_{12\nu} & -B_{14\nu} \\ -J'_\nu(u_1 r_1) & \frac{i\nu\beta}{\omega\mu_0 r_1} J_\nu(u_1 r_1) & -B_{22\nu} & -B_{24\nu} \\ 0 & u_1^2 J_\nu(u_1 r_1) & -B_{32\nu} & -B_{34\nu} \\ -\frac{i\nu\beta}{\omega\varepsilon_0 n_1^2 r_1} J_\nu(u_1 r_1) & -J'_\nu(u_1 r_1) & -B_{42\nu} & -B_{44\nu} \end{vmatrix}, \tag{35}$$

$$M_1 M_2^{-1} M_3 M_4^{-1} M_5 M_6^{-1} M_f = B_\nu, \tag{36}$$

$$B_\nu = \begin{pmatrix} 0 & B_{12\nu} & 0 & B_{14\nu} \\ 0 & B_{22\nu} & 0 & B_{24\nu} \\ 0 & B_{32\nu} & 0 & B_{34\nu} \\ 0 & B_{42\nu} & 0 & B_{44\nu} \end{pmatrix}. \tag{37}$$

In general, for a fiber with N layers the matrix elements for the layer just before the outermost region are

$$M_{2(N-2)-1} = M_1(r_1 \to r_{N-2}, u_2 \to u_{N-1}, n_2 \to n_{N-1}), \tag{38}$$

$$M_{2(N-2)-1,g} = M_1(r_1 \to r_{N-2}, u_2 \to u_{N-1}, n_2 \to n_{N-1}, J_\nu \to H_{1\nu}, \\ Y_\nu \to H_{2\nu}), \tag{39}$$

$$M_{2(N-2)} = M_1(r_1 \to r_{N-1}, u_2 \to u_{N-1}, n_2 \to n_{N-1}), \tag{40}$$

$$M_{2(N-2),g} = M_1(r_1 \to r_{N-1}, u_2 \to u_{N-1}, n_2 \to n_{N-1}, J_\nu \to H_{1\nu}, Y_\nu \to H_{2\nu}). \tag{41}$$

3. NUMERICAL RESULTS AND DISCUSSION

The analytical method is demonstrated in a hollow-core Bragg fiber, which is made by air in the center of the structure, surrounded by periodic reflector layers with large refractive-index contrast in the cladding. In addition, the high index material just before the outermost region of the fiber is replaced by a gold layer. Thus, the loss for the TE_{01} mode is decreased about ten times.

The optical properties of a Bragg fiber with a hollow-core of large radius and a large refractive-index contrast in periodic layers of the cladding, but without a gold layer were calculated in [12]. The fiber parameters were r = 13.02 µm, n_1 = 1, d_1 = 0.09444 µm, n_2 = 4.6, d_2 = 0.33956 µm, n_3 = 1.6, λ = 1.55 µm, and N = 19, where r is the radius of the core, n_1 is the refractive index of the air in the core, d_1 is the thickness of the layer with high refractive index n_2, d_2 is the thickness of the layer with low refractive index n_3, λ is the wavelength and N is the number of the layers.

By using the usual quarter wave condition:

$$d_1 = \frac{\lambda}{4\sqrt{n_2^2 - n_1^2}}, \; d_2 = \frac{\lambda}{4\sqrt{n_3^2 - n_1^2}}, \tag{42}$$

we have calculated the thickness d_1 = 0.086303 µm for the layer with high refractive index (n_2 = 4.6) and the thickness d_2 = 0.310248 µm for the layer with a low refractive index (n_3 =1.6) in the cladding structure, where n_1 = 1 is the refractive index in the core region (air). For the hollow-core Bragg fiber with N layers, r_1 =13.02 µm, n_1 = 1, $n_2 = n_4 = \ldots = n_{N-1}$ = 4.6, $n_3 = n_5 \ldots = n_N$ = 1.6. The refractive index of the gold layer is calculated by the Drude model [13].

Table 1 shows the values of the effective index β/k, loss α, propagation length L, and wavelength λ for a hollow-core Bragg fiber with N = 5, 11, and 19 layers, r_1 =13.02 µm, n_1 = 1, d_1 = 0.086303 µm, d_2 = 0.310248 µm, $n_2 = n_4 = \ldots = n_{N-1}$ = 4.6, $n_3 = n_5 \ldots = n_N$ = 1.6. The symbol * refers to d_1 = 0.086292 µm and

d_2 = 0.309726 µm computed with the quarter-wave stack condition in the case of infinite cladding pairs [14, 15]:

$$\frac{\lambda}{d_1} = 2\sqrt{4(n_2^2 - n_1^2) + (\frac{\lambda J_{1,1}}{\pi r_1})^2}\ ,\ \frac{\lambda}{d_2} = 2\sqrt{4(n_3^2 - n_1^2) + (\frac{\lambda J_{1,1}}{\pi r_1})^2}\ , \tag{43}$$

where $J_{1,1}$= 3.83170597 is the first root of the Bessel function J_1. If we approximate

$$\begin{aligned} 4(n_2^2 - n_1^2) + (\frac{\lambda J_{1,1}}{\pi r_1})^2 &\approx 4(n_2^2 - n_1^2) \\ 4(n_3^2 - n_1^2) + (\frac{\lambda J_{1,1}}{\pi r_1})^2 &\approx 4(n_2^2 - n_1^2), \end{aligned} \tag{44}$$

one obtains the usual quarter wave condition (42). The minimum-loss wavelength λ_{min} shifts ($\Delta\lambda$ = 20.8 nm for N =19, $\Delta\lambda$ = 40.4 nm for N = 11, and $\Delta\lambda$ = 128 nm for N = 5) toward a short wavelength as the number of the layers N becomes small.

Table 1

Values of the effective index β / k, loss α, propagation length L and wavelength λ for a hollow-core Bragg fiber with N layers, r_1 =13.02 µm, n_1 =1, d_1 = 0.086303 µm, d_2 = 0.310248 µm, $n_2 = n_4 = ... = n_{N-1}$ = 4.6, $n_3 = n_5 ... = n_N$ = 1.6

N	β / k (without gold)	α [dB/cm]	L [µm]	λ [µm]
5	0.997361 + 4.820915×10^{-7} i	1.697430×10^{-1}	2.558541×10^{5}	1.5500
5	0.997782 + 4.036744×10^{-7} i	1.549047×10^{-1}	2.803623×10^{5}	1.4222
11	0.997361 + 2.253839×10^{-10} i	7.935701×10^{-5}	5.472667×10^{8}	1.5500
11	0.997498 + 2.137121×10^{-10} i	7.726120×10^{-5}	5.621120×10^{8}	1.5096
19	0.997361 + 8.178485×10^{-15} i	2.879621×10^{-9}	1.508165×10^{13}	1.5500
19	0.997361 + 8.178337×10^{-15} i	2.879569×10^{-9}	1.508193×10^{13}	1.5500*
19	0.997432 + 7.962187×10^{-15} i	2.841596×10^{-9}	1.528347×10^{13}	1.5292
19	0.997432 + 7.948044×10^{-15} i	2.836548×10^{-9}	1.531067×10^{13}	1.5292*

Figure 1 shows the refractive index *versus* the radius of the layers for an air-core Bragg fiber with N = 5 when the layer just before the outermost region is a dielectric (n_4 = 4.6) or a gold material. Figure 2 shows a quarter of a cross section of the same fiber and a contour plot of the z-component $S_z(x, y)$ of the Poynting vector at the wavelength (λ = 1.4222 µm when n_4 = 4.6 and λ = 1.4188 µm when n_4 = 0.503628–8.838158i) of the fiber lowest loss for the TE_{01} mode. Figure 3 shows the loss spectra for the TE_{01} mode for the same fiber without a gold layer and with a gold layer. Figure 4 is similar to Fig. 1 but for $N = 19$. Figure 5 shows the real part of the effective index *versus* wavelength for the TE_{01} mode for a fiber with $N = 19$. Figure 6 is similar to Fig. 3 but for $N = 19$.

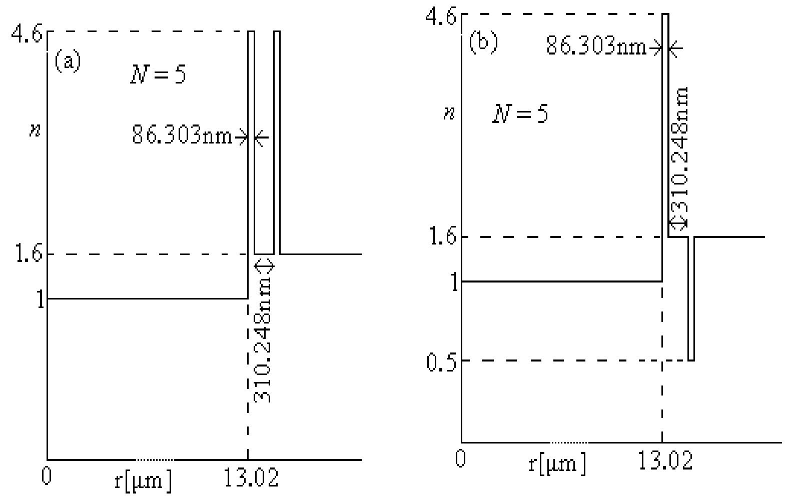

Fig. 1 – The refractive index *versus* the radius of the core and cladding layers when $n_4 = 4.6$ (a) and $n_4 = 0.503628–8.838158i$ (b) for an air-core Bragg fiber with $N = 5$.

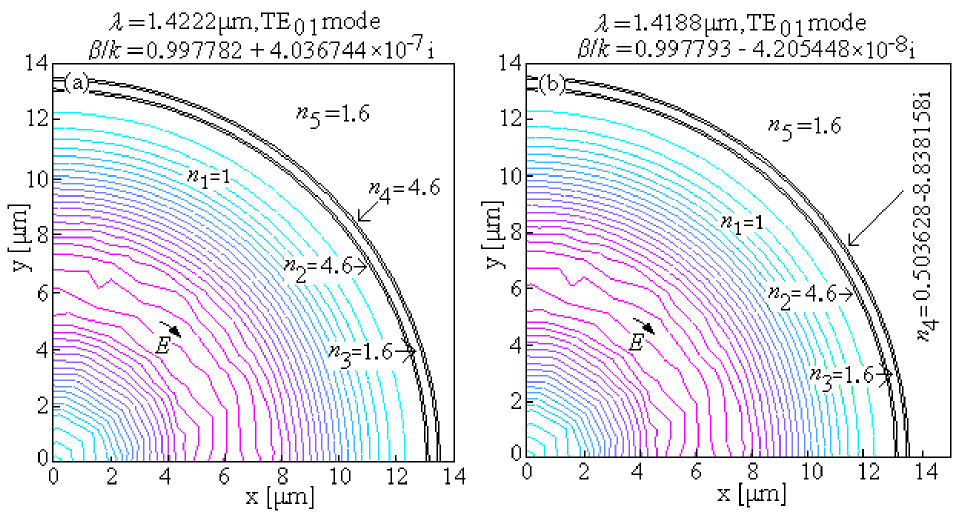

Fig. 2 – A quarter of a cross section of a hollow-core Bragg fiber with five layers and a contour plot of the z-component $S_z(x, y)$ of the Poynting vector at the wavelength $\lambda = 1.4222$ μm when $n_4 = 4.6$ (a) and $\lambda = 1.4188$ μm when $n_4 = 0.503628–8.838158i$ (b) of the fiber lowest loss for the TE_{01} mode. The main electric field E of the TE_{01} mode is parallel with the surface of the Bragg layers.

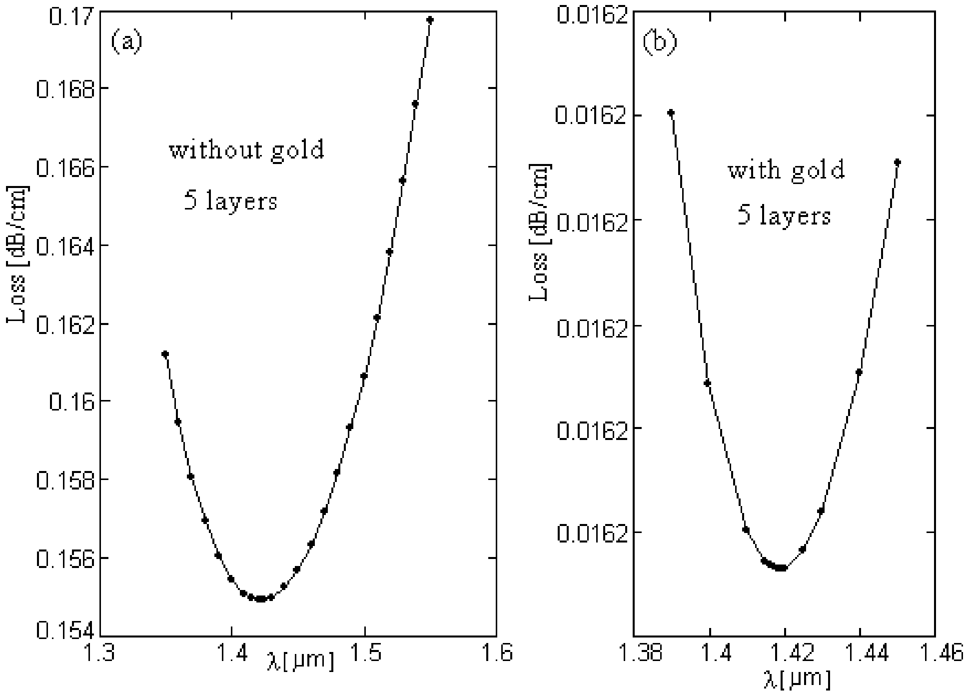

Fig. 3 – The loss spectra for the TE_{01} mode in an air-core Bragg fiber with $N = 5$, without a gold layer (a) and with a gold layer (b).

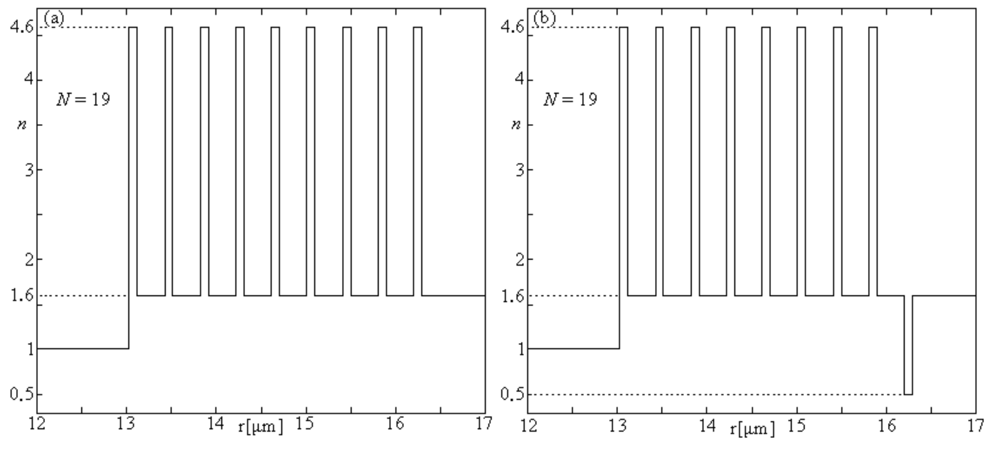

Fig. 4 – The refractive index *versus* the radius of the core and cladding layers when $n_{18} = 4.6$ (a) and $n_{18} = 0.503628–8.838158i$ (b) for an air-core Bragg fiber with $N = 19$.

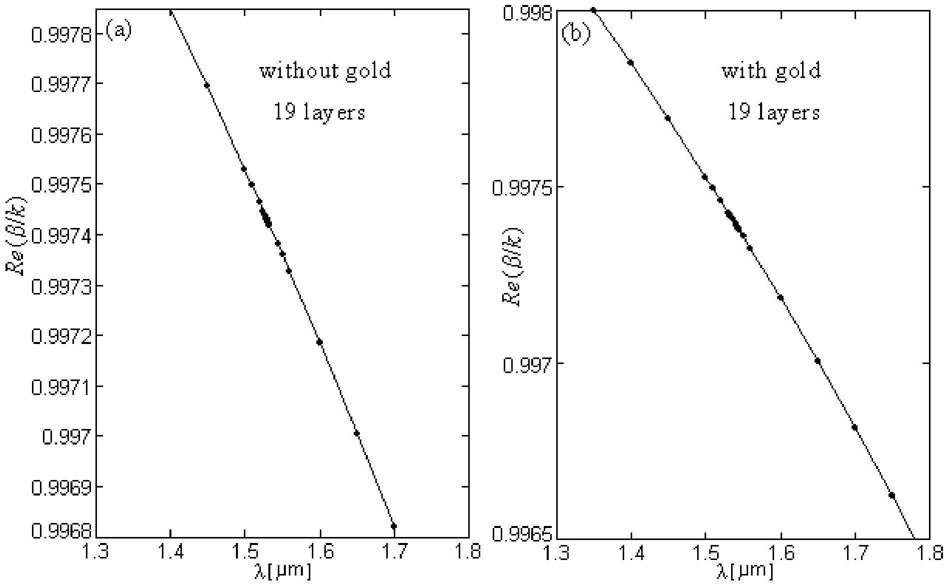

Fig. 5 – The real part of the effective index *versus* the wavelength for the TE_{01} mode for an air-core Bragg fiber with $N = 19$, without a gold (a) and with (b) a single gold (for n_{18}) layer.

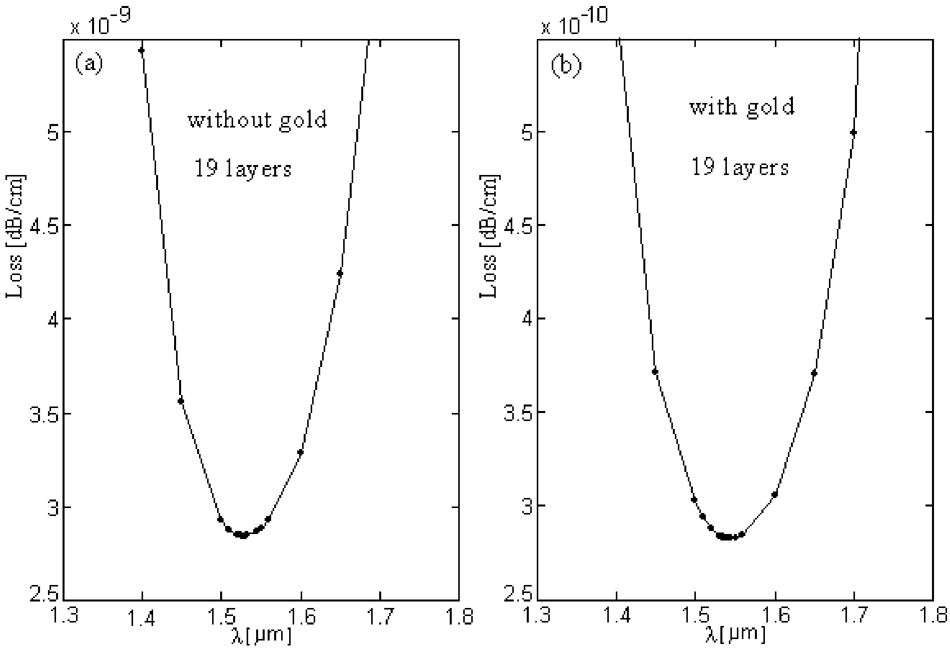

Fig. 6 – The loss spectra for the TE_{01} mode in an air-core Bragg fiber with $N = 19$, without a gold layer (a) and with a gold layer (b).

Table 2 shows the values of β / k, α, L and λ for a hollow-core Bragg fiber with N = 5, 11, and 19 layers, r_1 = 13.02 μm, n_1 = 1, d_1 = 0.086303 μm, d_2 = 0.310248 μm, $n_2 = n_4 = ... = n_{N-3}$ = 4.6, $n_{N-1} = n_{gold}$, $n_3 = n_5 ... = n_N$ = 1.6, when a high index material just before the outermost region is replaced by a gold layer.

The symbol * refers to d_1 = 0.086292 μm and d_2 = 0.309726 μm computed with the quarter-wave stack condition in the case of infinite cladding pairs. The minimum-loss wavelength λ_{min} shifts ($\Delta\lambda$ = 5.7 nm for N = 19, $\Delta\lambda$ = 13.6 nm for N = 11, and $\Delta\lambda$ = 131.2 nm for N = 5) toward a short wavelength as the number of the layers N becomes small.

Table 2

Values of β / k, α, L and λ for a hollow-core Bragg fiber with N layers, r_1 = 13.02 μm, n_1 = 1, d_1 = 0.086303 μm, d_2 = 0.310248 μm, $n_2 = n_4 = ... = n_{N-3}$ = 4.6, $n_{N-1} = n_{gold}$, $n_3 = n_5 ... = n_N$ = 1.6

N	β / k (with gold)	α [dB/cm]	L [μm]	λ [μm]
5	$0.997362 - 4.731900\times10^{-8}$ i	1.666089×10^{-2}	2.606671×10^{6}	1.5500
5	$0.997793 - 4.205448\times10^{-8}$ i	1.617653×10^{-2}	2.684720×10^{6}	1.4188
11	$0.997361 - 2.213349\times10^{-11}$ i	7.793137×10^{-6}	5.572781×10^{9}	1.5500
11	$0.997408 - 2.188955\times10^{-11}$ i	7.775472×10^{-6}	5.585442×10^{9}	1.5364
19	$0.997361 - 8.034501\times10^{-16}$ i	2.828925×10^{-10}	1.535193×10^{14}	1.5500
19	$0.997361 - 8.025363\times10^{-16}$ i	2.825707×10^{-10}	1.536941×10^{14}	1.5500*
19	$0.997381 - 7.995152\times10^{-16}$ i	2.825460×10^{-10}	1.537075×10^{14}	1.5443
19	$0.997381 - 7.985089\times10^{-16}$ i	2.821904×10^{-10}	1.539012×10^{14}	1.5443*

Table 3 shows the values of the loss α and amplitude sensitivity S_A for the TE_{01} mode for two values of the refractive index of the first (interior) and the last (exterior) layer for a hollow-core Bragg fiber with N = 19 layers, r_1 = 13.02 μm, n_1 = 1, d_1 = 0.086303 μm, d_2 = 0.310248 μm with and without gold.

Table 3

Values of the loss α and amplitude sensitivity S_A for the TE_{01} mode for two values of the refractive index of the first (interior) and the last (exterior) layer

N	n_1	n_{18}	n_{19}	α [dB/cm]	S_A [RIU^{-1}]	λ [μm]
19	1	4.6	1.6	2.841596×10^{-9}		1.5292
19	1	4.6	1.601	2.844500×10^{-9}	1.022	1.5292
19	1.001	4.6	1.6	2.808443×10^{-9}	–11.624	1.5291
19	1	0.572174–9.621939i	1.6	2.825460×10^{-10}		1.5443
19	1	0.572174–9.621939i	1.601	2.825433×10^{-10}	–0.00971	1.5443
19	1.001	0.572174–9.621939i	1.6	2.794629×10^{-10}	–10.912	1.5443

In the case without gold, the differences between the losses are: $\alpha\,(n_1 = 1) - \alpha\,(n_1 = 1.001) = 3.3153 \times 10^{-11}$ dB/cm and $\alpha\,(n_{19} = 1.6) - \alpha\,(n_{19} = 1.601) = -2.904 \times 10^{-12}$ dB/cm. In the case with gold, the differences between the losses are: $\alpha\,(n_1 = 1) - \alpha\,(n_1 = 1.001) = 3.0831 \times 10^{-12}$ dB/cm and $\alpha\,(n_{19} = 1.6) - \alpha\,(n_{19} = 1.601) = 2.7 \times 10^{-15}$ dB/cm.

Figure 7 shows the loss spectra for two values of the refractive index of the core layer ($n_a = 1$ and $n_a = 1.001$) and the amplitude sensitivity for the TE_{01} mode for an air-core Bragg fiber with $N = 19$, without a gold layer. In this case the maximum of the amplitude sensitivity is $S_A = -11.624$ RIU^{-1} at $\lambda = 1.5291$ µm.

Figure 8 is similar to Fig. 7 but for the case with a gold layer. The maximum of the amplitude sensitivity is $S_A = -10.912$ RIU^{-1} at $\lambda = 1.5443$ µm.

Figure 9 is similar to Fig. 7 but for two values of the refractive index of the exterior layer ($n_a = 1.6$ and $n_a = 1.601$). The maximum of the amplitude sensitivity is only $S_A = 1.022$ RIU^{-1} at $\lambda = 1.5292$ µm.

Figure 10 is similar to Fig. 9 but for the case with a gold layer. In this case the maximum of the amplitude sensitivity is smaller ($S_A = -0.00971$ RIU^{-1} at $\lambda = 1.5443$ µm).

Figure 11 shows the loss *versus* the thickness t_g of the gold layer in $n_{layer} = 5$ for the TE_{01} mode in an air-core Bragg fiber with $N = 6$. One observe that optical confinement for the TE_{01} mode in the core is increased (the loss is decreased) with the thickness of the gold layer.

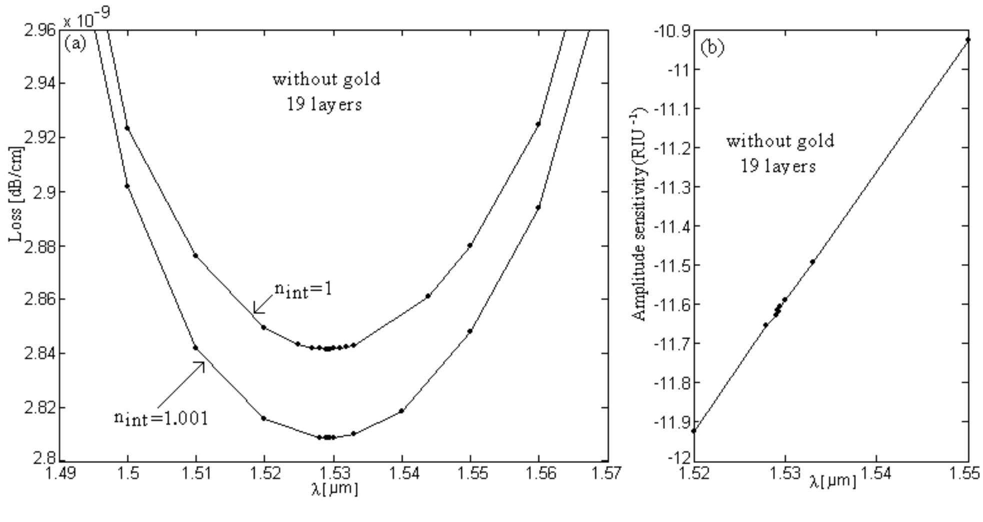

Fig. 7 – The loss spectra (a) for two values of the analyte (interior) refractive index ($n_a = 1$ and $n_a = 1.001$) and the amplitude sensitivity (b) for the TE_{01} mode for an air-core Bragg fiber with $N = 19$, without a gold layer.

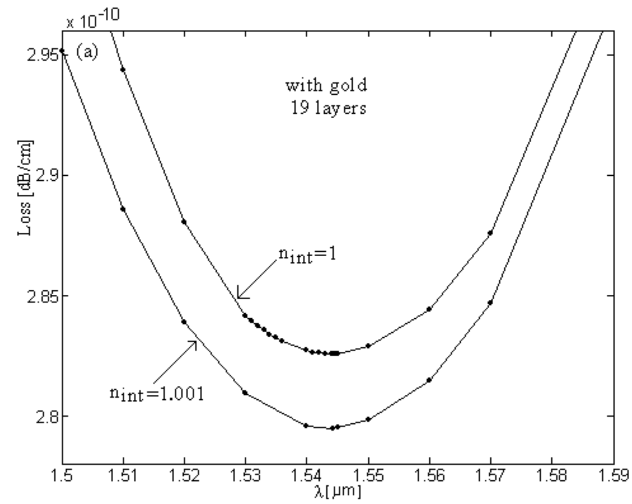

Fig. 8 – The loss spectra (a) for two values of the analyte (interior) refractive index ($n_a = 1$ and $n_a = 1.001$) and the amplitude sensitivity (b) for the TE_{01} mode for an air-core Bragg fiber with $N = 19$, with a single gold layer.

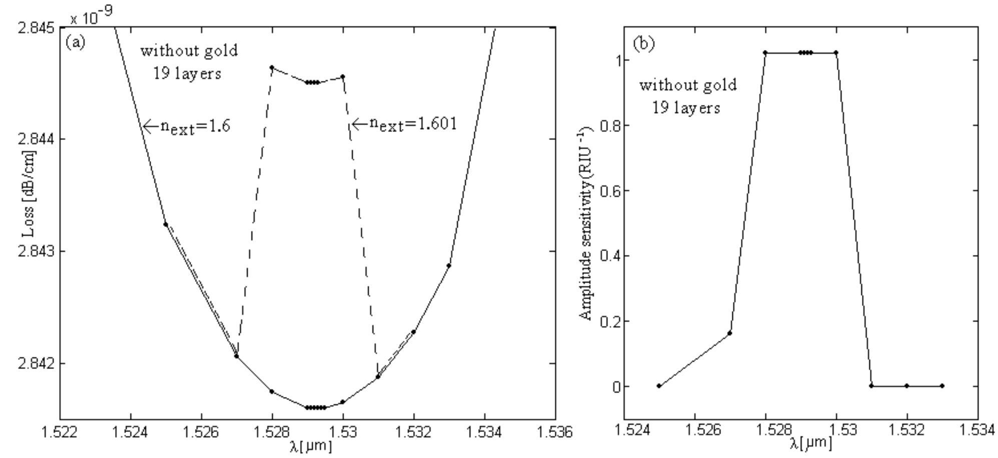

Fig. 9 – The loss spectra (a) for two values of the analyte (exterior) refractive index ($n_a = 1.6$ and $n_a = 1.601$) and the amplitude sensitivity (b) for the TE_{01} mode for an air-core Bragg fiber with $N = 19$, without a gold layer.

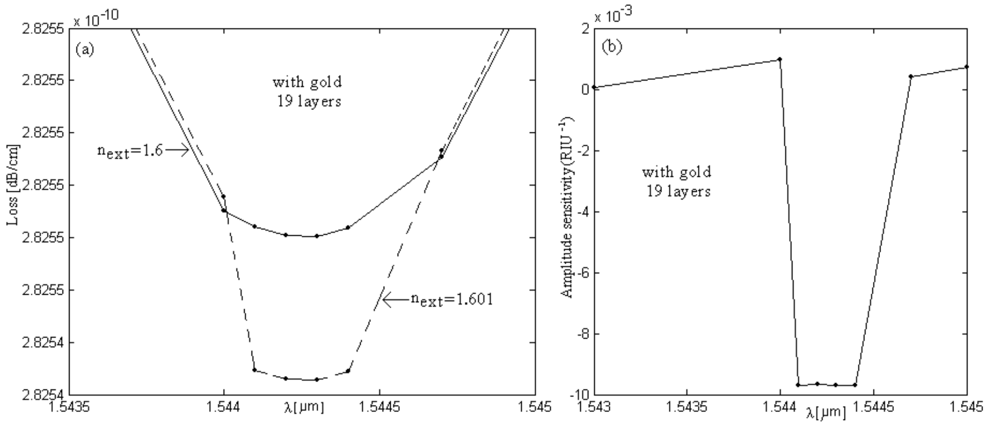

Fig. 10 – The loss spectra (a) for two values of the analyte (exterior) refractive index (n_a = 1.6 and n_a = 1.601) and the amplitude sensitivity (b) for the TE_{01} mode for an air-core Bragg fiber with N = 19, with a single gold layer (N = 18).

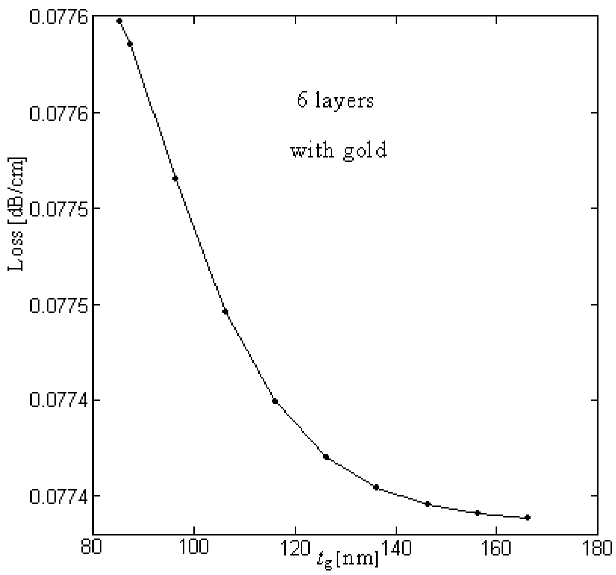

Fig. 11 – The loss *versus* the thickness t_g of the gold layer in N = 5 for the TE_{01} mode in an air-core Bragg fiber with N = 6.

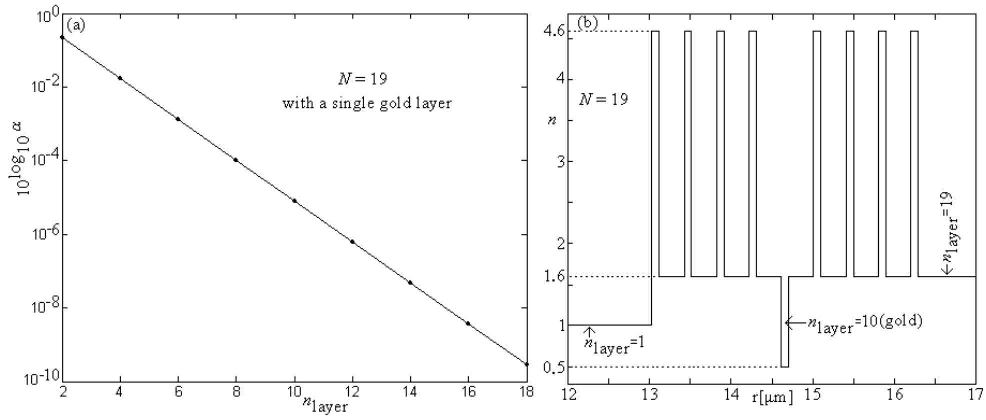

Fig. 12 – a) The loss in the logarithmic scale (base 10) *versus* the number n_{layer} of the gold layer, where α is in dB/cm; b) the refractive index *versus* the radius of the core and cladding layers when $n_{\text{layer}} = 10$.

Figure 12 shows the loss in the logarithmic scale *versus* the number n_{layer} of the gold layer and the refractive index *versus* the radius of the layers when $n_{\text{layer}} = 10$.

If the gold layer is located between the first and the penultimate layer, the loss for the same mode is increased. Table 4 shows the values of the effective index β/k, loss α, and propagation length L for an air-core Bragg fiber with N = 19 layers, r_1 =13.02 μm, n_1 =1, d_1 = 0.086303 μm, d_2 = 0.310248 μm, λ = 1.55 μm, when the gold layer is located between the first and the last layer.

Table 4

Values of β/k, α, and L for a hollow-core Bragg fiber with N = 19 layers, r_1 = 13.02 μm, n_1 = 1, d_1 = 0.086303 μm, d_2 = 0.310248 μm, λ = 1.55 μm, when the gold layer is located between the first and the last layer with n_{layer} = 2, 4, 6, 8, 10,12, 14, 16, and 18

n_{layer}	β/k (with gold)	α [dB/cm]	L [μm]
2	$0.997371 - 6.114745\times10^{-7}$ i	2.152984×10^{-1}	2.017174×10^{5}
4	$0.997762 - 4.774691\times10^{-8}$ i	1.681155×10^{-2}	2.583310×10^{6}
6	$0.997361 - 3.707468\times10^{-9}$ i	1.305389×10^{-3}	3.326936×10^{7}
8	$0.997361 - 2.877559\times10^{-10}$ i	1.013180×10^{-4}	4.286449×10^{8}
10	$0.997361 - 2.233364\times10^{-11}$ i	7.863610×10^{-6}	5.522839×10^{9}
12	$0.997361 - 1.733384\times10^{-12}$ i	6.103194×10^{-7}	7.115855×10^{10}
14	$0.997361 - 1.345284\times10^{-13}$ i	4.736706×10^{-8}	9.168703×10^{11}
16	$0.997361 - 1.043499\times10^{-14}$ i	3.674130×10^{-9}	1.182033×10^{13}
18	$0.997361 - 8.034501\times10^{-16}$ i	2.828925×10^{-10}	1.535193×10^{14}

4. CONCLUSION

When a high index material just before the outermost region of a hollow-core Bragg fiber is replaced by a gold layer, the optical confinement for the TE_{01} mode in the core is increased about ten times for any number of layers. A very good optical confinement is obtained for a large number of the layers. Also, the optical confinement for the TE_{01} mode in the core is increased (the loss is decreased) with the thickness of the gold layer and if the thickness of the cladding layers are computed with the quarter-wave stack condition in the case of infinite cladding pairs.

For the same wavelength, the real parts of the effective indices β / k for the hollow-core Bragg fiber with or without gold layer are the same and for large number of layers can be approximated with the value given by the relation [16]:

$$\mathrm{Re}(\beta / k) \approx \sqrt{n_1^2 - \left(\frac{J_{1,1}\lambda}{2\pi r_1}\right)^2}\ , \tag{45}$$

where $J_{1,1}$ is the same as in the relation (43). Thus, for r_1 = 13.02 μm, n_1 = 1 and λ = 1.55 μm, $\mathrm{Re}(\beta / k)$ = 0.9973611820, as in Tables 1–2. Also, for the same r_1 and n_1 but for λ = 1.5292 μm, $\mathrm{Re}(\beta / k)$ = 0.9974316199 as in Table 1. On the other hand, the imaginary part of the effective index β / k is very sensitive to the number of the layers and if the structure is with or without a gold layer.

If the gold layer is located between the first and the penultimate layer, the loss for the same TE_{01} mode is increased because the parts before and after the reflector gold layer of the fiber are decoupled.

Our method is in good agreement with the data known from the literature in the case of a hollow-core Bragg fiber without a gold layer. Thus for a hollow-core Bragg fiber with N = 34 layers (32 reflector layers, 16 pairs), r_1 = 1.3278 μm, n_1 = 1, d_1 = 0.2133 μm, d_2 = 0.346 μm, $n_2 = n_4 = \ldots = n_{34}$ = 1.49, $n_3 = n_5 \ldots = n_{33}$ = 1.17, λ = 1 μm, our effective index for the TE_{01} mode β / k = 0.8910672175 + $1.4226046712 \times 10^{-8}$i is very close to the calculated value in Ref. [17], β / k = 0.891067 + 1.4226 $10^{-8}\, i$.

When a high index material just before the outermost region of a hollow-core Bragg fiber is replaced by a gold layer, the optical confinement for the TE_{01} mode in the core is increased about ten times. Thus, the light of a high power laser can be transmitted with very low loss due to the large confinement in the core of the fiber.

REFERENCES

1. J. Chilwell and I. Hodgkinson, J. Opt. Soc. Am. A **1**, 742 (1984).
2. C. Yeh and G. Lindgren, Appl. Optics **16**, 483 (1977).
3. C. Y. H. Tsao, J. Opt. Soc. Am. A **6**, 555 (1989).
4. S. R. Dods, *Integrated Photonics Research and Applications*, Paper ITuF5, DOI: doi.org/10.1364/IPRA.2006.ITuF5 (2006).
5. V. A. Popescu, J. Supercond. Nov. Magn. **25**, 1413 (2012).
6. Z. Zang, Appl. Optics **52**, 5701 (2013).
7. Z. Zang and Y. Zhang, Appl. Optics **51,** 3424 (2012).
8. V. A. Popescu, N. N. Puscas, and G. Perrone, Mod. Phys. Lett. B **30**, 1650075 (2016).
9. V. A. Popescu, N. N. Puscas, and G. Perrone, Plasmonics **11**, 1183 (2016).
10. V. A. Popescu, Rom. J. Phys. **62**, 204 (2017).
11. V. A. Popescu and N. N. Puscas, Rom. Rep. Phys. **67**, 500 (2015).
12. S. Johnson, M. Ibanescu, M. Skorobogatiy, O. Weisberg, T. Engeness, M. Soljacic, S. Jacobs, J. Joannopoulos, and Y. Fink, Opt. Express **9**, 748 (2001).
13. A. D. Rakić, A. B. Djurišić, J. M. Elazar, and M. L. Majewski, Appl. Opt. **37**, 5271 (1998).
14. J. Sakai, J. Opt. Soc. Am. B **22**, 2319 (2005).
15. J. Sakai and H. Niiro, Opt. Express **16**, 1885 (2008).
16. A. Argyros, Opt. Express **10**, 1411 (2002).
17. I. M. Bassett and A. Argyros, Opt. Express **10**, 1342 (2002).